Machine Learning Many-Body Localization: Search for the Elusive Nonergodic Metal

Yi-Ting Hsu,[1,*] Xiao Li,[1,†] Dong-Ling Deng,[1,2] and S. Das Sarma[1]
[1]*Condensed Matter Theory Center and Joint Quantum Institute, University of Maryland, College Park, Maryland 20742, USA*
[2]*Institute for Interdisciplinary Information Sciences, Tsinghua University, Beijing, China, 100084*

(Received 6 June 2018; revised manuscript received 21 September 2018; published 10 December 2018)

The breaking of ergodicity in isolated quantum systems with a single-particle mobility edge is an intriguing subject that has not yet been fully understood. In particular, whether a nonergodic but *metallic* phase exists or not in the presence of a one-dimensional quasiperiodic potential is currently under active debate. In this Letter, we develop a neural-network-based approach to investigate the existence of this nonergodic metallic phase in a prototype model using many-body entanglement spectra as the sole diagnostic. We find that such a method identifies with high confidence the existence of a nonergodic metallic phase in the midspectrum at an intermediate quasiperiodic potential strength. Our neural-network-based approach shows how supervised machine learning can be applied not only in locating phase boundaries but also in providing a way to definitively examine the existence or not of a novel phase.

DOI: 10.1103/PhysRevLett.121.245701

Introduction.—Investigating the properties of eigenstates in isolated quantum many-body systems is essential for understanding dynamical phases and their transitions, and even more importantly, the very question of thermal equilibrium in quantum statistical mechanics. In the noninteracting limit, the single-particle orbitals of a fermionic system throughout the energy spectrum can be all localized [1], all extended, or exhibit a single-particle mobility edge (SPME) [2–13] separating localized and extended states. The SPME is in fact thought to be the generic situation for three-dimensional disordered systems. Moreover, the existence of a SPME in an incommensurate one-dimensional (1D) system has recently been predicted and experimentally observed in a quasiperiodic optical lattice [14,15].

In the presence of interactions, we can further introduce the notion of ergodicity for a many-body eigenstate since a closed quantum system can thermalize according to the eigenstate thermalization hypothesis (ETH) [16–18]. Since the critical energies for the localization and thermalization transitions do not necessarily coincide, more complicated phases can occur other than all eigenstates being many-body localized (MBL) [19–41], i.e., localized and nonergodic, or all obeying the ETH, i.e., extended and ergodic. In particular, recent numerical studies have found that in systems subject to a family of incommensurate potentials that exhibit SPME, there exists a finite energy window wherein the eigenstates are nonergodic but extended [34–36]. Such an intriguing intermediate phase was subsequently named the nonergodic metal (NEM) [35].

The common strategy taken by prior studies to identify NEM [34–36] was to detect localization and ergodicity by different diagnostics. This was necessary since different phases are naturally more sensitive to different diagnostics, which is also true in the experimental studies of MBL [42–45]. The problem with this strategy is that these *ad hoc* different diagnostics may not necessarily be equivalent with respect to their sensitivity to various phases. For instance, while entanglement entropy and the variance in local particle number fluctuations were used to diagnose localization and ergodicity in Ref. [35], the inverse participation ratio and the return probability were used in Ref. [34] along with several other diagnostics. Since the energy window for NEM is set by the two transition energies corresponding to the two distinct diagnostics, the phase space or even the existence of NEM itself can largely depend on the combination of the diagnostics used, which is unsatisfactory. In order to definitively establish NEM as a phase with a finite phase space in the phase diagram, it is imperative to develop an approach that can distinguish MBL, NEM, and the thermal states (ETH states) using a single diagnostic.

The entanglement spectrum (ES) [46] is an appealing choice in this context because of the following reasons. First, the ES contains more information about the eigenstates than entanglement entropy due to the absence of the tracing procedure. Second, recent studies have identified the ES as a sensitive probe for MBL and ETH phases [47–51]. However, the complexity of the spectral pattern in an ES makes it practically difficult to extract relevant features for discerning eigenstate properties.

Machine learning, a powerful tool for complex pattern recognition, has recently been introduced to condensed matter physics and raised tremendous interest in the community [52–69]. In particular, supervised learning has been used as a successful numerical tool to study various phases and their transitions [52–55]. One such application is to identify the phase boundaries throughout the parameter space using a neural-network (NN) classifier

trained with data obtained from well-known limits deep in each phase [48,52,70,71]. Such an approach, however, relies on *a priori* knowledge of all existing phases in the parameter space, which is not always available. To the best of our knowledge, studies in this direction have so far been limited to models where the existence of all phases are well established without controversies, which is not suitable for our goal of investigating the presence of the controversial NEM phase whose very existence as an intermediate phase between ETH and MBL remains open.

In this Letter, we develop a general NN approach targeting a different goal from that of conventional supervised learning to examine the existence of a controversial phase. Using this novel approach, we investigate the dynamical phases in a prototype incommensurate 1D lattice model [35] emphasizing the existence of the NEM phase. Using the ES as the input data, we show that a three-layer NN is able to unambiguously identify a distinct new phase between the MBL and ETH phases with high confidence. Our results provide the strongest numerical evidence so far for the existence of a new phase in incommensurate systems that is likely the predicted NEM in Ref. [35] and also usher in a general machine-learning-based new technique for identifying novel phases of matter which may not be accessible by conventional techniques.

Model and method.—The model we study is the generalized Aubry-Andre (GAA) model [13] $H = H_0 + H_{\rm int}$ in a 1D system of size L, where

$$H_0 = \sum_{j=1}^{L}\left(-t(c_j^\dagger c_{j+1} + \text{H.c.}) + 2\lambda\frac{\cos(2\pi q j+\phi)}{1-\alpha\cos(2\pi q j+\phi)}n_j\right),$$
$$H_{\rm int} = V\sum_{j=1}^{L} n_{j+1}n_j. \quad (1)$$

Here, $n_j = c_j^\dagger c_j$ is the fermionic number operator at site j, V is the nearest-neighbor interaction strength, and t is the nearest-neighbor hopping strength as well as the energy unit throughout the article. The second term in H_0 describes an incommensurate potential with strength 2λ, an irrational wave number $q = 2/(1+\sqrt{5})$, a randomly chosen global phase ϕ, and a dimensionless parameter $\alpha \in (-1, 1)$.

The $\alpha = 0$ limit of Eq. (1) corresponds to the pristine AA model [72], which does not have a SPME. For the general $\alpha \neq 0$ case, however, a SPME generally exists at $V = 0$. Here we choose $\lambda = 0.3$ and $\alpha = -0.8$ to achieve a comparable number of localized and extended single-particle orbitals at $V = 0$ [35]. As reported in Ref. [35], the interacting many-body spectrum at some fixed λ may exhibit the NEM phase in a finite energy window $E_L < E < E_T$, whereas the MBL and ETH phases have energies $E < E_L$ and $E > E_T$, respectively. The important question we study in this work using our NN approach is the existence of the NEM phase in the interacting GAA model in the intermediate energy window.

We now describe how we build an M-phase classifier based on a candidate phase diagram that contains M phases, which serves as the building block of our NN approach. The network structure of the classifier contains an input layer, a hidden layer, and an output layer [Fig. 2(a)]. The size of the input layer is determined by the size of the input data, and the hidden layer contains 30 sigmoid neurons. The output layer contains N softmax neurons, and each produces a real number $p_i \in [0, 1], i = 1, \ldots, M$, with $\sum_{i=1}^{M} p_i = 1$. Thus, each output p_i can be viewed as the confidence the classifier identifies the input data as belonging to the phase i. We generate the input data by calculating the ES of the interacting GAA model using exact diagonalization with a varying global phase ϕ and a fixed particle number $N = L/6$. The training data set for each phase i is generated from one energy bin [73] labeled by E_i, $(i = 1, \ldots, M)$ deep in each phase i according to the assumed phase diagram we have in mind.

During the training process, we feed the training data to the input layer and allow the all-to-all couplings between the adjacent layers to evolve from randomly chosen initial values according to the log-likelihood cost function. We then test the trained network with another independent set of testing data obtained in the same way. If the training is successful, which we define as obtaining a testing accuracy over 99%, we feed the trained network with the ES from all energy bins throughout the spectrum in order to obtain the resulting phase diagram, which contains energy-resolved confidence $p_i(E)$, $i = 1, \ldots, M$.

The NN approach.—We develop a recursive procedure that consists of systematically building different classifiers starting from a candidate phase diagram to be tested, and telling from the outputs of these classifiers the correct number of phases. The technique is powerful enough to identify both falsely positive (incorrectly identifying a nonexisting phase) and falsely negative (not identifying an existing phase) cases. Here we first demonstrate our general approach using a toy example, where we associate each "phase" with a set of images of a handwritten digit from the MNIST database [74], a canonical source of input data sets for benchmarking machine learning algorithms. To better connect to the dynamical phase diagram of interest in this work, we present the results of this example by "phase diagrams" consisting of different digits. To mimic the continuous tuning parameter in usual phase diagrams, we divide the testing data for each digit into groups and plot the output of the network against the group labels.

First imagine a case where the studied phase space contains only phases A and B, but we falsely assume that a phase C exists in between. To test our assumption, we start by training a three-phase classifier with data obtained from small regimes within the phase spaces of A, B, as well as a phase space that we thought to be C but is actually a part of

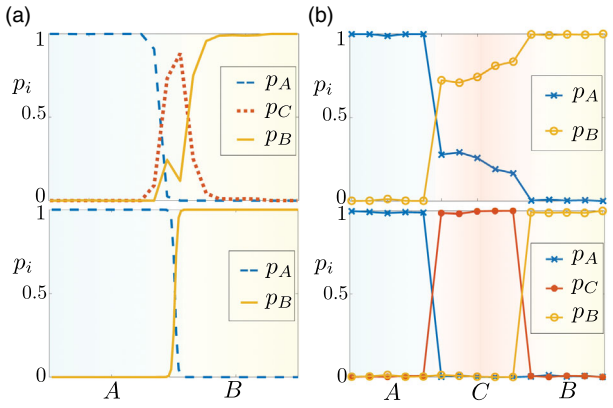

FIG. 1. Schematic results from applying our NN approach to toy examples identifying (a) a falsely assumed phase C in a system with only two phases A and B, and (b) an unnoticed hidden phase C in a system with three phases A, B, and C. (a) shows schematics illustrating situations described in the text, where the upper panel shows the falsely positive result produced by a three-phase classifier for A, B, and C, and the lower panel shows the correct result produced by a two-phase classifier for A and B. (b) shows results from calculation using MNIST data as input, where we associate A, B, and C with digits 1, 6, and 3, respectively. The upper panel shows the falsely negative result produced by a two-phase classifier for only A and B. The lower panel shows the correct result produced by a three-phase classifier for A, B, and C. Each tick on the horizontal axis corresponds to a group of 160 MNIST images of the associated digit. In both plots, p_i is the confidence for identifying certain input data as phase $i = A$, B, C, and the horizontal axis with background color blue, yellow, and red correspond to phase A, B, and C, respectively.

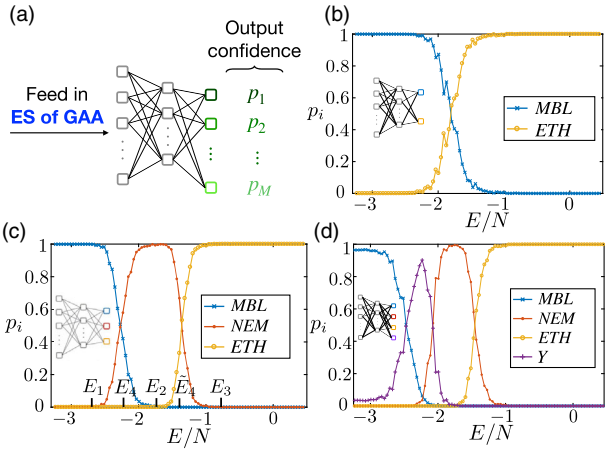

FIG. 2. (a) The schematics of the building block in our NN approach, a general M-phase classifier for phase $i = 1, \ldots, M$. The phase diagrams of the GAA model with $L = 30$ sites, potential strength $\lambda = 0.3$, and interaction strength $V = 1$ produced by (b) a two-phase classifier, (c) a three-phase classifier, and (d) a four-phase classifier. Here, $p_i(E)$ is the energy-dependent confidence at which the corresponding classifier identifies the eigenstates to be in each of the studied phases. The training data for the classifiers are collected from energy bins $E_1, \ldots, E_4$ and $\tilde{E}_4$ labeled in (c) for corresponding phases as discussed in the text.

B. Two scenarios can happen in this case. First, for simpler phases with a low variance within each phase, the training procedure itself would fail with low testing accuracy. Our example based on MNIST data falls in this category. Second, for more complicated phases with a large variance within each phase, the training process could be successful, but the regime identified as phase C with a high confidence ($p_C \to 1$) would be negligible or (at best) similar in size to the small regime where the training data for C were collected. This is because instead of capturing universal properties of a phase, the network is actually trained to capture detailed features tied to the small training regime. We show a schematic in the upper panel of Fig. 1(a) illustrating this second scenario, where the narrowly peaked confidence curve p_C and the apparent confusion between B and C suggests that there are fewer phases in reality than what we assumed. This is in contrast to the phase diagram produced by a two-phase classifier for A and B [bottom panel in Fig. 1(a)] that matches the reality, where each curve exhibits high confidence over a substantial phase space.

The above guidelines for identifying a falsely assumed phase can be further exploited to identify hidden phases. Now imagine another case where a phase C exists between phases A and B, but we only know of the latter two. To avoid overlooking any hidden phases, we perform the following recursive three-step procedure. Step I, we train a two-phase classifier for phases A and B. Step II, we apply the previous guideline to the resulting phase diagram [top panel of Fig. 1(b)] and find that neither of the confidence curves p_A and p_B is narrowly peaked, which indicates that both A and B phases exist. Step III, we assume some hidden phase C to exist within the regime where neither p_A nor p_B is high, and build a three-phase classifier accordingly. By reapplying step II to the resulting phase diagram [bottom panel of Fig. 1(b)], we again find that all three phases exist. When we further repeat step III to build a four-phase classifier assuming some phase D to exist between A and C or between C and B; however, the low testing accuracy in the training process suggests that phase D does not exist. We thus conclude that there exist only three phases A, B, and C as shown in the bottom panel of Fig. 1(b).

Results.—We now employ our NN approach to study the phase diagram of the GAA model in a system with $L = 30$ sites, fixed potential strength $\lambda = 0.3$, and interaction strength $V = 1$. First for step I, we assume that the many-body spectrum only consists of MBL near the band edges and ETH in the midspectrum, and no additional phases in between. Based on this assumption, we train a two-phase classifier with data collected from energies deep in the MBL (E_1) and ETH (E_3) phases [Fig. 2(c)], respectively. We find that while the resulting phase diagram [Fig. 2(b)] shows two substantial energy regimes identified

as MBL and ETH, respectively, there is also a substantial regime in between where the network does not show high confidence in identifying it as either.

Next for step II, we investigate whether there is a third phase X hidden in this transition regime by a three-phase classifier for MBL, ETH, and this phase X which we assume to exist. To do so, we train a three-phase classifier for MBL, ETH, and X with data collected from energy bins E_1, E_3, and E_2 [Fig. 2(c)], respectively. We then benchmark it against the well-known AA model and find the classifier to be reliable [75]. Applying this three-phase classifier to the GAA case, we find three substantial energy regimes identified as MBL, phase X, and ETH, respectively, with a high confidence as energy increases from the edge to the middle of the spectrum [Fig. 2(c)]. We emphasize that such a result strongly supports the existence of this third phase X under the lens of the ES since (i) the training process is successful with a testing accuracy over 99%, and (ii) the width of the identified phase X regime (with over 95% confidence) is 7 times wider than the size of the energy bin from which the training data for phase X were produced.

Before moving on to step III, we first comment on the properties of this phase X. First note that the phase diagram obtained from the three-phase classifier using a single diagnostic qualitatively agrees with that obtained using two diagnostics in Ref. [35]. In particular, the energy range for phase X in our results is slightly smaller but fully contained in that of NEM found in Ref. [35]. Therefore, the phase X we found here is most likely nonergodic while metallic; hence we will refer to this intermediate phase as NEM in the following. Moreover, the ES spectral pattern of the eigenstates we identified as NEM is qualitatively different from that of the MBL and ETH states [75]. This indicates that instead of being merely a mixture of MBL and ETH states over a small energy window, the NEM states are actually distinct types of eigenstates that are distinguishable from the MBL and ETH states by ES patterns.

Finally, for step III, we examine if we overlooked any additional hidden phases in the MBL-to-NEM and NEM-to-ETH transition regimes. We first train a four-phase classifier for MBL, NEM, ETH, and a fourth phase Y between MBL and NEM with data collected from energy bins at E_1, E_2, E_3, and E_4, respectively [Fig. 2(c)]. From the resulting phase diagram in Fig. 2(d), we find that the confidence curve of phase Y narrowly peaks at the training bin E_4, and no energy regime can be identified as phase Y with confidence over 90%. These observations suggest that phase Y does not exist, in sharp contrast to the results from the three-phase classifier, where we found a wide energy regime identified as NEM with high confidence [Fig. 2(a)]. We also find that there exists no hidden phases between NEM and ETH by performing a similar calculation replacing phase Y with a phase $\tilde{Y}$ between NEM and ETH, where the training data are collected from $\tilde{E}_4$ [75]. Thus, we predict that the actual phase diagram is the one

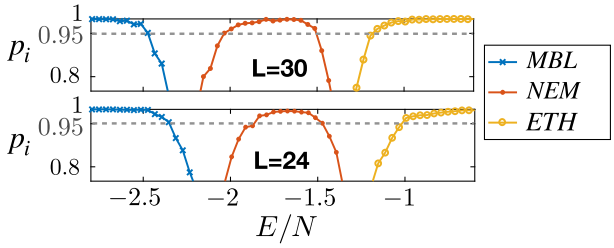

FIG. 3. The comparison between the $L = 30$ (upper) and $L = 24$ (lower) phase diagrams of the GAA model focused on the NEM regimes. Here the parameter choices are the same as those in Fig. 2.

produced by the three-phase classifier in Fig. 2(c), which supports the existence of NEM but no additional hidden phases.

After establishing the existence of NEM in the $L = 30$ system, we further investigate its stability under finite-size effects. We build a three-phase classifier for the $L = 24$ interacting GAA model, benchmark it against the interacting AA model [75], and use it to study the resulting phase diagram. We find that the regime identified as NEM with over 95% confidence increases by 40% as L increases from 24 to 30 [Fig. 3(b)]. Moreover, for the $L = 18$ case, we even fail to achieve a successful training process under a reasonable hyperparameter scan. The above observations are both consistent with the NEM regime becoming more robust as L increases. Furthermore, although studying any interacting systems with size $L > 30$ is not feasible under our current supercomputer resources, a finite-size analysis in the noninteracting limit can provide additional hints on the robustness of the NEM phase [75]. Based on our interacting and noninteracting studies, we conclude that it is extremely unlikely that our unbiased identification of the NEM phase as distinct from MBL or ETH phases can be a finite-size artifact.

Conclusion.—We have developed a neural-network-based method for determining the existence of a novel dynamical quantum phase near many-body localization transition, which is an application of supervised machine learning beyond locating phase boundaries among existing phases. Our method allows one to detect hidden phases or, conversely, identify false hypothetical phases by systematically building different neural-network classifiers. By using this technique, we have established that interacting 1D incommensurate systems with single-particle mobility edges may contain a still-not-very-well-understood nonergodic but metallic phase in the midenergy spectrum. Such a phase has an ES spectral pattern very distinct from that of MBL and ETH. We have shown that the technique is highly reliable with confidence levels for various identified phases reaching $> 99\%$ even using ES data from systems rather modest in size. We mention that our method is related to Ref. [53] in that the requirement of *a prior* knowledge of the phase diagram is minimized. Meanwhile, our technique focuses on uncovering hidden

phases in systems with multiple phases. Our technique is general and should be applicable to both equilibrium and nonequilibrium quantum problems.

The authors acknowledge helpful discussions with Jordan Venderley, Shenglong Xu, Xiaopeng Li, and Brian Swingle. This work is supported by Microsoft and Laboratory for Physical Sciences. The authors acknowledge the University of Maryland supercomputing resources made available for conducting the research reported in this Letter.

Y.-T. H. and X. L. contributed equally to this work.

*ythsu@umd.edu
†lixiao@umd.edu

[1] P. W. Anderson, Phys. Rev. **109**, 1492 (1958).
[2] N. Mott, *Metal-Insulator Transitions* (CRC Press, Boca Raton, 1990).
[3] C. M. Soukoulis and E. N. Economou, Phys. Rev. Lett. **48**, 1043 (1982).
[4] P. A. Lee and T. V. Ramakrishnan, Rev. Mod. Phys. **57**, 287 (1985).
[5] S. D. Sarma, A. Kobayashi, and R. E. Prange, Phys. Rev. Lett. **56**, 1280 (1986).
[6] M. Griniasty and S. Fishman, Phys. Rev. Lett. **60**, 1334 (1988).
[7] S. D. Sarma, S. He, and X. C. Xie, Phys. Rev. Lett. **61**, 2144 (1988).
[8] D. J. Thouless, Phys. Rev. Lett. **61**, 2141 (1988).
[9] S. D. Sarma, S. He, and X. C. Xie, Phys. Rev. B **41**, 5544 (1990).
[10] D. J. Boers, B. Goedeke, D. Hinrichs, and M. Holthaus, Phys. Rev. A **75**, 063404 (2007).
[11] J. Biddle and S. D. Sarma, Phys. Rev. Lett. **104**, 070601 (2010).
[12] J. Biddle, D. J. Priour, B. Wang, and S. D. Sarma, Phys. Rev. B **83**, 075105 (2011).
[13] S. Ganeshan, J. H. Pixley, and S. D. Sarma, Phys. Rev. Lett. **114**, 146601 (2015).
[14] X. Li, X.-P. Li, and S. D. Sarma, Phys. Rev. B **96**, 085119 (2017).
[15] H. P. Lüschen, S. Scherg, T. Kohlert, M. Schreiber, P. Bordia, X. Li, S. D. Sarma, and I. Bloch, Phys. Rev. Lett. **120**, 160404 (2018).
[16] J. M. Deutsch, Phys. Rev. A **43**, 2046 (1991).
[17] M. Srednicki, Phys. Rev. E **50**, 888 (1994).
[18] M. Rigol, V. Dunjko, and M. Olshanii, Nature (London) **452**, 854 (2008).
[19] I. V. Gornyi, A. D. Mirlin, and D. G. Polyakov, Phys. Rev. Lett. **95**, 206603 (2005).
[20] D. Basko, I. Aleiner, and B. Altshuler, Ann. Phys. (Amsterdam) **321**, 1126 (2006).
[21] V. Oganesyan and D. A. Huse, Phys. Rev. B **75**, 155111 (2007).
[22] M. Žnidarič, T. Prosen, and P. Prelovšek, Phys. Rev. B **77**, 064426 (2008).
[23] A. Pal and D. A. Huse, Phys. Rev. B **82**, 174411 (2010).
[24] J. H. Bardarson, F. Pollmann, and J. E. Moore, Phys. Rev. Lett. **109**, 017202 (2012).
[25] S. Iyer, V. Oganesyan, G. Refael, and D. A. Huse, Phys. Rev. B **87**, 134202 (2013).
[26] R. Nandkishore and D. A. Huse, Annu. Rev. Condens. Matter Phys. **6**, 15 (2015).
[27] R. Nandkishore, Phys. Rev. B **92**, 245141 (2015).
[28] D. J. Luitz, N. Laflorencie, and F. Alet, Phys. Rev. B **93**, 060201 (2016).
[29] J. Z. Imbrie, J. Stat. Phys. **163**, 998 (2016).
[30] J. A. Kjäll, J. H. Bardarson, and F. Pollmann, Phys. Rev. Lett. **113**, 107204 (2014).
[31] D. J. Luitz, N. Laflorencie, and F. Alet, Phys. Rev. B **91**, 081103 (2015).
[32] I. Mondragon-Shem, A. Pal, T. L. Hughes, and C. R. Laumann, Phys. Rev. B **92**, 064203 (2015).
[33] M. Serbyn, Z. Papić, and D. A. Abanin, Phys. Rev. X **5**, 041047 (2015).
[34] R. Modak and S. Mukerjee, Phys. Rev. Lett. **115**, 230401 (2015).
[35] X.-P. Li, S. Ganeshan, J. H. Pixley, and S. D. Sarma, Phys. Rev. Lett. **115**, 186601 (2015).
[36] X.-P. Li, J. H. Pixley, D.-L. Deng, S. Ganeshan, and S. D. Sarma, Phys. Rev. B **93**, 184204 (2016).
[37] K. Hyatt, J. R. Garrison, A. C. Potter, and B. Bauer, Phys. Rev. B **95**, 035132 (2017).
[38] E. Baygan, S. P. Lim, and D. N. Sheng, Phys. Rev. B **92**, 195153 (2015).
[39] E. J. Torres-Herrera and L. F. Santos, Ann. Phys. (Berlin) **529**, 1600284 (2017).
[40] D. J. Luitz, Phys. Rev. B **93**, 134201 (2016).
[41] S. Nag and A. Garg, Phys. Rev. B **96**, 060203 (2017).
[42] M. Schreiber, S. S. Hodgman, P. Bordia, H. P. Luschen, M. H. Fischer, R. Vosk, E. Altman, U. Schneider, and I. Bloch, Science **349**, 842 (2015).
[43] P. Bordia, H. P. Lüschen, S. S. Hodgman, M. Schreiber, I. Bloch, and U. Schneider, Phys. Rev. Lett. **116**, 140401 (2016).
[44] J. y. Choi, S. Hild, J. Zeiher, P. Schauss, A. Rubio-Abadal, T. Yefsah, V. Khemani, D. A. Huse, I. Bloch, and C. Gross, Science **352**, 1547 (2016).
[45] J. Smith, A. Lee, P. Richerme, B. Neyenhuis, P. W. Hess, P. Hauke, M. Heyl, D. A. Huse, and C. Monroe, Nat. Phys. **12**, 907 (2016).
[46] H. Li and F. D. M. Haldane, Phys. Rev. Lett. **101**, 010504 (2008).
[47] S. D. Geraedts, R. Nandkishore, and N. Regnault, Phys. Rev. B **93**, 174202 (2016).
[48] F. Schindler, N. Regnault, and T. Neupert, Phys. Rev. B **95**, 245134 (2017).
[49] J. Venderley, V. Khemani, and E.-A. Kim, Phys. Rev. Lett. **120**, 257204 (2018).
[50] Z.-C. Yang, C. Chamon, A. Hamma, and E. R. Mucciolo, Phys. Rev. Lett. **115**, 267206 (2015).
[51] M. Serbyn, A. A. Michailidis, D. A. Abanin, and Z. Papić, Phys. Rev. Lett. **117**, 160601 (2016).
[52] J. Carrasquilla and R. G. Melko, Nat. Phys. **13**, 431 (2017).
[53] E. P. van Nieuwenburg, Y.-H. Liu, and S. D. Huber, Nat. Phys. **13**, 435 (2017).
[54] K. Ch'ng, J. Carrasquilla, R. G. Melko, and E. Khatami, Phys. Rev. X **7**, 031038 (2017).

[55] N. Yoshioka, Y. Akagi, and H. Katsura, Phys. Rev. B **97**, 205110 (2018).
[56] G. Carleo and M. Troyer, Science **355**, 602 (2017).
[57] D.-L. Deng, X. Li, and S. D. Sarma, Phys. Rev. B **96**, 195145 (2017).
[58] L. Wang, Phys. Rev. B **94**, 195105 (2016).
[59] L.-F. Arsenault, O. A. von Lilienfeld, and A. J. Millis, arXiv:1506.08858.
[60] D.-L. Deng, X. Li, and S. D. Sarma, Phys. Rev. X **7**, 021021 (2017).
[61] S. J. Wetzel, Phys. Rev. E **96**, 022140 (2017).
[62] W. Hu, R. R. P. Singh, and R. T. Scalettar, Phys. Rev. E **95**, 062122 (2017).
[63] X. Gao and L.-M. Duan, Nat. Commun. **8**, 662 (2017).
[64] Y. Huang and J. E. Moore, arXiv:1701.06246.
[65] J. Chen, S. Cheng, H. Xie, L. Wang, and T. Xiang, Phys. Rev. B **97**, 085104 (2018).
[66] Z. Cai and J. Liu, Phys. Rev. B **97**, 035116 (2018).
[67] F. Schindler, N. Regnault, and T. Neupert, Phys. Rev. B **95**, 245134 (2017).
[68] P. Broecker, F. F. Assaad, and S. Trebst, arXiv:1707.00663.
[69] Y. Nomura, A. S. Darmawan, Y. Yamaji, and M. Imada, Phys. Rev. B **96**, 205152 (2017).
[70] Y. Zhang and E.-A. Kim, Phys. Rev. Lett. **118**, 216401 (2017).
[71] P. Broecker, J. Carrasquilla, R. G. Melko, and S. Trebst, Sci. Rep. **7**, 8823 (2017).
[72] S. Aubry and G. André, Ann. Isr. Phys. Soc. **3**, 133 (1980).
[73] The generated ES data are sorted into a series of energy bins with a width of $0.04t$, which constitute the unit of energy throughout the rest of this Letter. We have checked that the size of these energy bins is sufficiently small for ensuring convergence of our numerics.
[74] Y. LeCun and C. Cortes, NIST, http://yann.lecun.com/exdb/mnist/.
[75] See Supplemental Material at http://link.aps.org/supplemental/10.1103/PhysRevLett.121.245701 for discussions about AA model, perspectives from non-interacting GAA model, entanglement spectra of GAA model, and numerical details.